Modeling of MFL System to Inspect Ferro Magnetic Tubes

M. Prabhakaran
PG Student
National Engineering College
Kovilpatti

P. Karuppasamy
Full Time Research Scholar
National Engineering College
Kovilpatti

A. Abudhahir, Ph.D
Professor and Head / EIE
National Engineering College
Kovilpatti

B. P. C. Rao, Ph.D
Head, EMSI Section, NDE Division
Indira Gandhi Centre for Atomic Research
Kalpakkam

ABSTRACT
This paper expounds the 3D modelling of the MFL imaging system to monitoring the outer surface defects in Ferro-magnetic Steam Generator Tube (SGT). It features a new flaw detection technique in conjunction with the Magnetic Flux Leakage (MFL) inspection and Digital Imaging. It delivers information of the defective tube surface in the form of a digital image. The impact of variation in the dimension of flaws on the MFL signal is additionally analysed for enhancing the reliability of detection of various defect characteristics. Modelling of MFL imaging system has been done using COMSOL 4.3 for prediction of leakage fields of defective SGT.

General Terms
Modelling and Simulation

Keywords
Magnetic Flux Leakage , Steam Generator Tube, Digital Imaging, COMSOL 4.3, 3D Modelling, Defect Characterisation.

1. INTRODUCTION
Pipe line transportation is a widely used methodology which transports raw materials like oil, steam gas etc., to the plant. The Steam Generator (SG) is a significant constituent, wherein nuclear heat is transferred from molten sodium to water to produce steam in a sodium cooled reactor. The Steam Generator Tubes (SGTs), which are the heart of the atomic plant, are a bunch of pipelines used to generate the steam gas to the plant. The SGT is a critical component owing to the fact that both sodium and steam co-exist and can react viciously in case of any direct contact. The SGTs are revealed to a broad variety of climatic conditions, from sub-zero temperatures to high temperature desert conditions. Doubtless, dangerous flaws are flat bottom holes, notches, wall thinning, pitting, wearing and cracking flaws in both the inner and outer surface of the tube [1]. Any leakage which occurs on the SGT, either due to aging or other catastrophic failures, will certainly cause ecological and economic hazards for the plant.

Quite a few researches have reported a number of MFL techniques for the detection and characterisation of the defects for steel plates and large diameter tubes [2-12]. It utilises yoke arrangement to magnetise the test specimen. Machine learning techniques were used to detect the defects by signal processing algorithm like principal component analysis, vector regression, partial least squares and kernalization [13-16]. Machine learning reduces the burden of the NDT technician, however, it requires a complex analysis algorithm for detection of defects and to check the severity of the defects. 3D modelling, as reported in previous attempts were done by the Finite Element Method (FEM), which evaluates the defects only for ferromagnetic plates [17-19]. Recently, 3D modelling and simulation of the MFL signal based defect detection system using COMSOL have been proposed [20-22]. They evaluated the defect identification in plates by analysing only the MFL signal.

In this present work, a 3D MFL based imaging system has been modelled to detect the outer surface defects (rectangular notch) of the SGTs (ID=12.6 mm; OD=17.2 mm; length=100 mm) using COMSOL 4.3. The proposed model employs a bobbin coil arrangement to generate uniform magnetic field for the smaller region of the tube. The leakage flux in the proximity of the defect region has been detected and used for image construction. The defects which appeared in the resultant images conform to the shapes and dimensions of the defects made in the geometry. The outcomes of the present study revealed that this proposed MFL imaging system would be very useful to detect the minute depth (10% of the wall thickness of the tube) defects.

We also discussed the impact of defect variation like length and width. The MFL is analysed in two broad classes specifically, the MFL analysed by signal and the MFL by means of image. The results are used to determine repair and replacement priorities of the SGT depending upon the flaw severity. Typically, a defect is identified by a simulated strip of sensors [23] placed along the axis of the tube. Once the defects have been identified, an equally vital problem is the assessment of the size or the severity of defect. For this, we introduced the construction of image from model predicted flux leakage field. In this paper, we propose imaging system for defect detection and produce high resolution image of defected portion to grasp the severity of the defect using a simulated MFL signal.

From this valid information, the database for the different types of flaw characteristics can be maintained. Current rating and depth variations may lead to modelling any Ferro-magnetic tubes of different diameter and length.

The organisation of this paper is as follows: background of MFL technique, proposed flaw detection technique, simulation analysis, results and discussions and finally, the conclusion.

2. BACKGROUND OF MFL TECHNIQUE

Permanent magnet or electro magnet magnetises the pipe to saturation or near saturation flux density, generally in the axial direction. Flux excitation in the circumferential direction is also possible. In the presence of defects within the SGT, it acts as a localised magnetic dipole with effective magnetic moment opposite to the applied magnetic field. This leads to a proportion of the flux leaking out of the material surface. This phenomenon is known as Magnetic Flux Leakage (MFL).This discharge of flux is detected by magnetic sensors and used to extract the information of defected surface. Hence, a saturated magnetic field around the SGT is an important criterion to be considered.

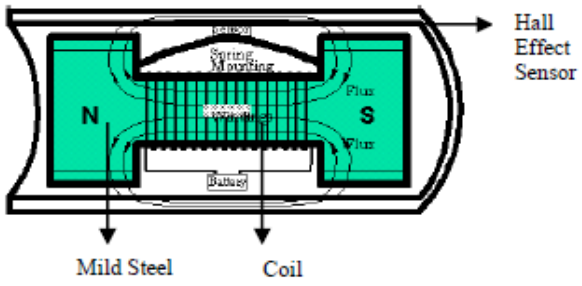

Fig 1: Schematic representation of MFL by bobbin coil arrangement

Bobbin coil arrangement with DC excitation produces saturated magnetic field and able to find sub-surface defects [3]. Hence, we prefer bobbin coil arrangement to magnetise the SGT. Figure 1 shows the schematic representation of the MFL by bobbin coil arrangement.

3. PROPOSED FLAW DETECTION TECHNIQUE

The major steps of the modelled MFL imaging system are shown in Figure 2. Here modelling and simulation of SGT has been done by COMSOL 4.3, and, the subsequent imaging has been done by MATLAB R2011a.

Bobbin coil magnetises the pipe wall to a saturated level while it travels down the pipe. Defects in the pipe wall cause irregularities in the magnetic field, which are detected by an array of magnetic sensors, placed at regular intervals around the circumference of the pipe wall. The simulated sensors points [23] are placed in close proximity with the inside surface of the pipe wall for optimum sensitivity to flux variation.

Here 64 simulated sensor points (cut point [23]) are used to measure the localised MFL intensity along the pipe wall for every scan, and those values are stored separately. Once the entire tube has been scanned, then the task of constructing the image will be fairly simple with the aid of an appropriate imaging technique.

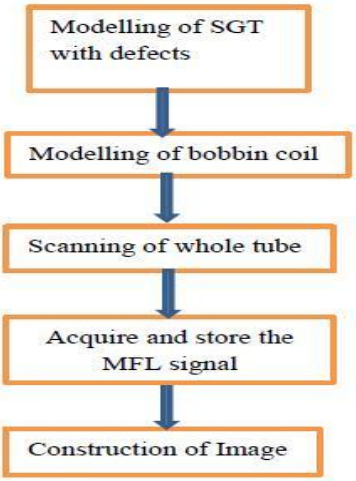

Fig 2: Modeling of proposed MFL imaging system

During the process of scanning, sensor points and bobbin are moved together step by step to avoid the non-uniformity of scanning. A matrix array of size M×N has been obtained; where M denotes number of rows which is an indication of linear motion of the bobbin and sensor arrangement, and N denotes number of columns, which is an indication of the array of circumferential sensor points.

By introducing the different artificial notches of different shapes and sizes on the surface of the tube, a number of MFL images were constructed and analysed.

4. SIMULATION ANALYSIS

4.1 3D Model of SGT

COMSOL 4.3 MULTIPHYSICS (AC/DC module) Software [23] is used for 3D finite element modelling. Figure 3 shows the geometry of bobbin coil arrangement. And, Figure 4 shows the front view of the Steam Generator Tube (SGT) and bobbin coil arrangement.

In order to obtain the experimental results, 3D modelling is preferable. Figure 5 indicates the 3D geometry of the SGT and bobbin coil arrangement.

The SGT has 100 mm length, 2.3 mm wall thickness, Inner Diameter (ID) and Outer Diameter (OD) of the tube is 12.6 mm and 17.2 mm respectively. The bobbin arrangement shown in Figure 3 has 50 mm length and the coil wound around the bobbin has 26 mm length, 3.8 mm thickness and number of turns 100 with 1A DC bias.

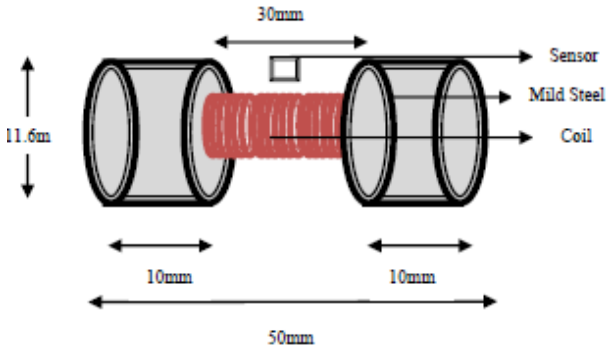

Fig 3: Geometry of bobbin coil arrangement with Hall Effect sensor

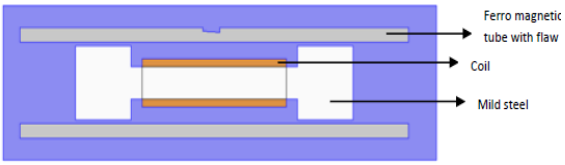

Fig 4: Front view of SGT and bobbin coil arrangement

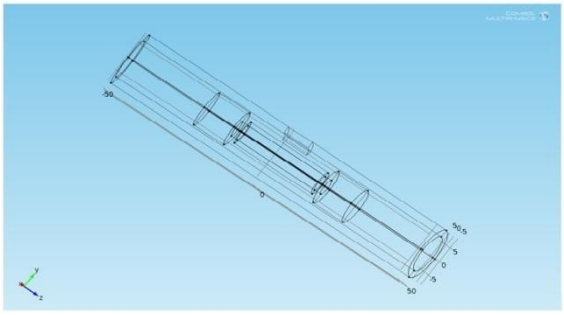

Fig 5: 3D Geometry of tube and bobbin coil arrangement

TABLE 1. Material properties of tube and bobbin coil arrangement

s.no	Material property	Material		
		9 Chromium – 1Molybdenum	Mild steel	copper
1	Relative permittivity	1	1	1
2	Electrical conductivity [S/m]	4.032e6	59.6e6	5.9998e7
3	Relative permeability	100	250	1

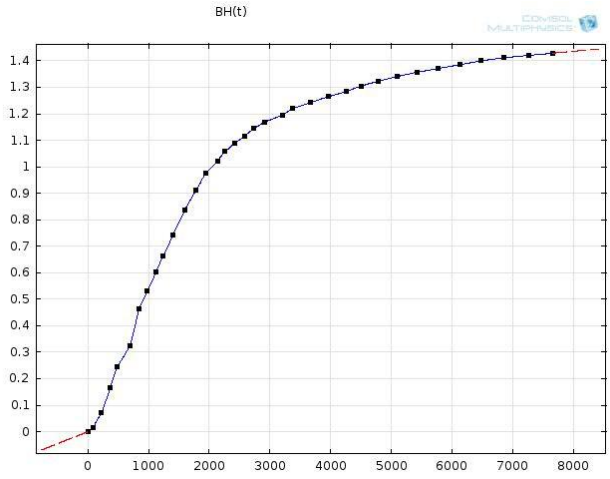

Fig 6: B-H curve details of SGT

Another important point here is the import of the B-H curve value of SGT in order to simulate better results. The B-H curve detail of the SGT obtained from IGCAR, Kalpakkam is shown in fig.6. It indicates that the field intensity, H, will be saturated at particular B value. The material properties of each domain have been listed in Table 1. Generally, the permeability, conductivity and permittivity are the parameters required to simulate the real time system.

4.2 Governing Equation to Solve the MFL System

Maxwell's equations are applicable to the analysis of electric as well as magnetic field within the MFL systems. Treating MFL problem as magneto-static, the following equations (1-5) have been used with usual notation.

$$\nabla . B = 0 \tag{1}$$

$$\nabla \times H = J \tag{2}$$

$$B = \nabla \times A \tag{3}$$

$$B = \mu H \tag{4}$$

$$B = \mu_{0(H+M)} \tag{5}$$

Assuming the magnetic permeability of the SGT as isotropic, equation (2) can be written as

$$\nabla \times \left(\frac{1}{\mu} \nabla \times A \right) = J \tag{6}$$

Equation (6) is solved in three dimensions using the FE (Finite Element) method.

Where,

A - The vector magnetic potential,

H - The magnetic field intensity,

B - The magnetic flux density,

J - The current density,

ρ - The electric charge density.

5. RESULTS AND DISCUSSIONS

A number of simulations were carried out in order to evaluate the performance of the developed MFL imaging system. The SGT containing different geometry of defect with various length and width was used as a test specimen. In order to measure the magnetic flux density distribution, norm B component of flux density was used. While the bobbin scanned the SGT, the reading records of flux density were being stored in a cumulative manner, and displayed in the form of images using MATLAB script. These results obtained have been discussed in following passages. The following Figures 6(a) and 6(b), illustrate the Magnetic Flux Leakage (MFL) profile obtained while simulating the modelled MFL system. The various simulation studies and analyses made in this work are listed below.

- Comparing the resultant signal of flux leakage for defective and non-defective portions.

- Obtain the flux leakage profile for various shape of defect geometry (rectangular and triangular).

- By placing multiple cut point (single sensor) [3] in circumferential manner around the bobbin, then traversing the bobbin coil arrangement and obtain matrix of data, then constructing the image.

These investigations yield the information required to maintain the database. Once the database has formulated from the MFL signal modelling, the fabrication of a practical system becomes simple.

5.1 Analysis by MFL signal

5.1.1 Flux Leakage for Defective and Non-Defective Portions

Figure 6a demonstrates the flux leakage for the flawed and the flawless portion. Generally, a notch is placed on the origin. For the flawless portion, the maximum value of magnetic flux density is 9800 G which is sensed by cutline [23], whereas, for the flawed portion, it is 12200 G. The Cutline graph holds the valid information for different notches and their corresponding flux leakage.

5.1.2 Flux Leakage Profile for the Triangular Shape of Defect

Figure 6b demonstrates the magnetic flux density leakage while varying the shape of the defect. Here, the shape of the defect is triangular (equilateral triangle of side 2.55 mm).

It is evident that the flux leakage profile highly depends on the shape of the defect. By comparing the peak portion of Figure 6b with Figure 6a, it is inferred that if the notch is rectangular, then the peak portion is flat in structure, whereas for the triangular defect, the plot is shown like an apex in the top. These plots provide valid information regarding defect characterisation.

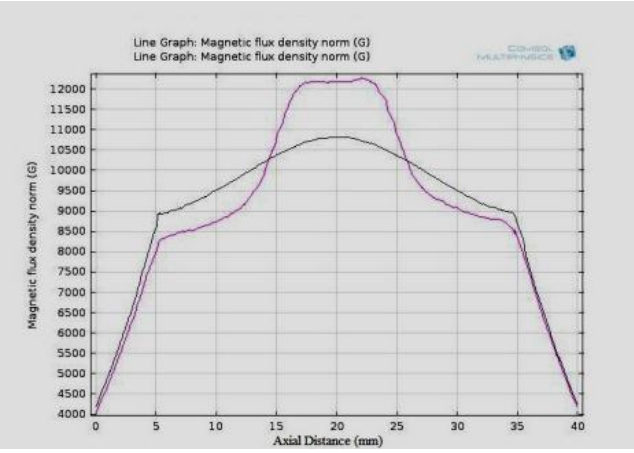

Fig 6a: Magnetic flux density leakage for with and without defect.

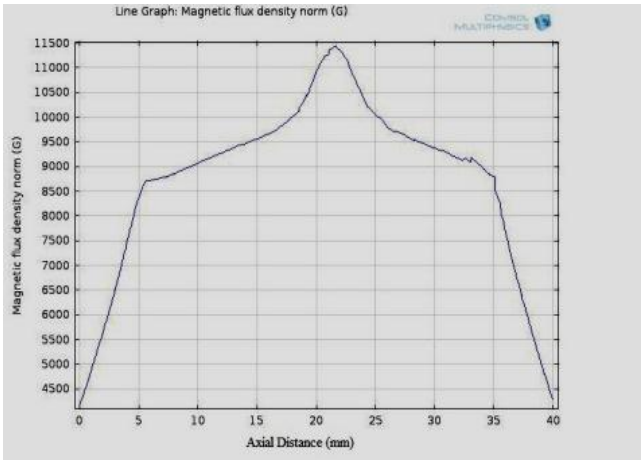

Fig 6b: Magnetic flux density leakage while varying the shape of the defect, here the shape of the defect is triangular (equilateral triangle of 2.55 mm).

5.2 Imaging Results

In order to construct an image, the bobbin coil assembly with cut points [23] is moved step by step along the axial distance. The flux density read at each cut point is stored against its spatial coordinates in an array.

The spatial resolution of the image depends upon the number of cut points placed along the circumference of the tube and distance moved in each step. This is done by placing multiple cut point (simulated sensor point) in a circumferential manner around the bobbin, then the linear scanning of the tube is done by bobbin coil arrangement for every 1mm step along the z axis (-25 mm to 25 mm) .

The tube has been imaged by keeping

- Depth and width of the defect constant for varying length

- Length and depth of the defect constant for varying width

5.2.1 Length Variation with Constant Width and Depth

Figure 7a shows the tube surface for the 8mm length of rectangular notch. The simulation of the MFL signal analysis concludes that if the defect length is increased, its magnitude (peak value) does not vary; only the variation belongs to the size of defective portion signal.

Figure 7b shows the tube surface for the 16 mm length of rectangular notch. When compared with previous figures, it shows the change of length in a linear manner, without any variation in the intensity value of the defect.

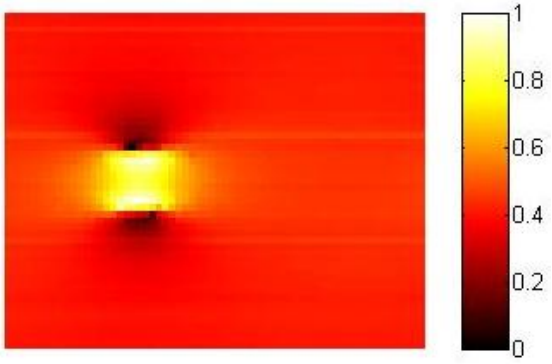

Fig 7a: Image of the defective tube surface for 8mm length of rectangular notch

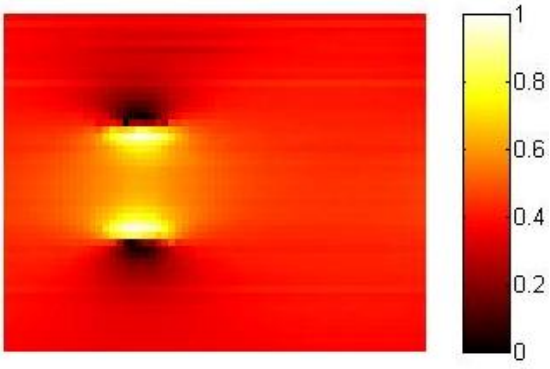

Fig 7b: Image of the defective tube surface for 16mm length of rectangular notch

5.2.2 Width Variation with Constant Depth and Length

Figure 8a illustrates that the defective tube surface for 60^o revolve (9.005 mm width) of rectangular notch. It is important to note that while increasing the width of the defect, the intensity of the image will vary.

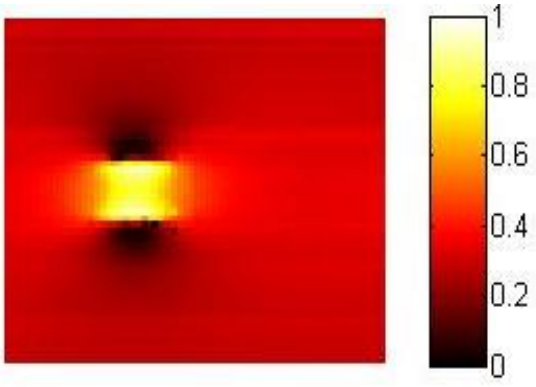

Fig 8a: Image of the defective tube surface for 9.005 mm width of rectangular notch

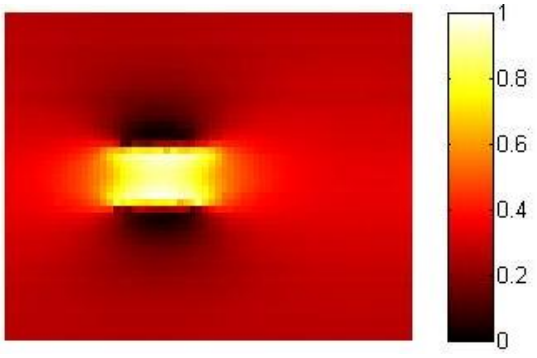

Fig 8b: Image of the defective tube surface for 13.5088 mm width of rectangular notch

Figure 8b illustrates that the defective tube surface for 90^o revolve, while keeping length and depth of the defect constant. It is one quarter of the perimeter of the tube. If one considers folding the image, it looks like the defected tube with the angle start from 0 to 90^o.

Plot for Depth Variation

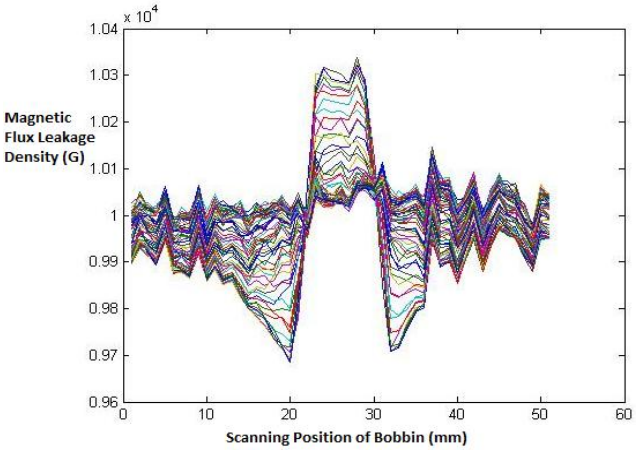

Fig 9a: Leakage profile for 0.23 mm depth

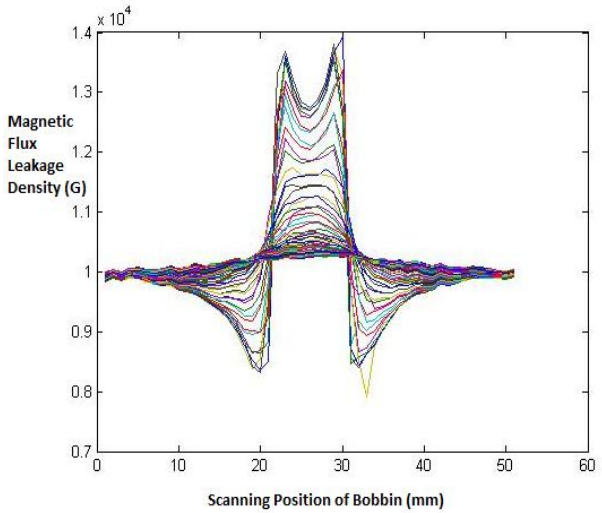

Fig 9b: Leakage profile for 1.4 mm depth

Plot for Width Variation

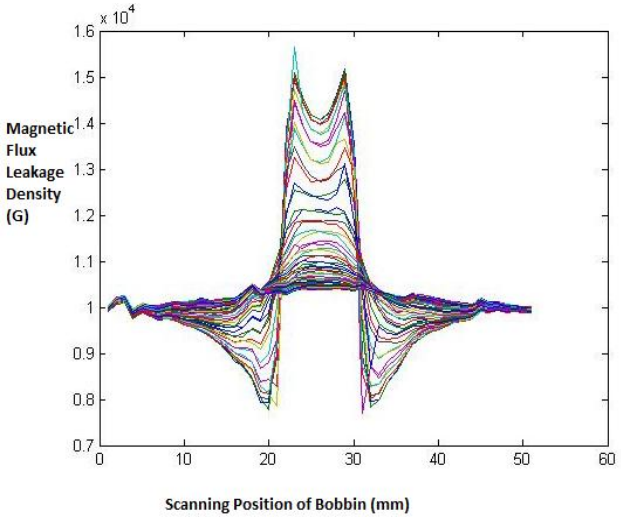

Fig 9c: Leakage profile 60° (9.005 mm) width

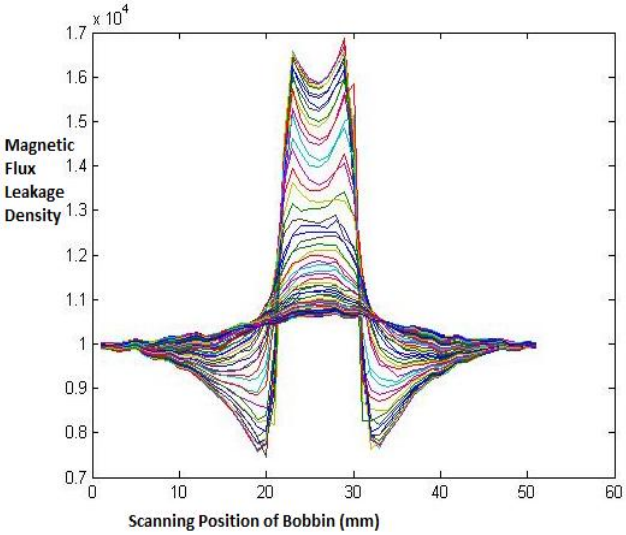

Fig 9d: Leakage profile for 90° (13.508 mm) width

Surface Plot for length variation

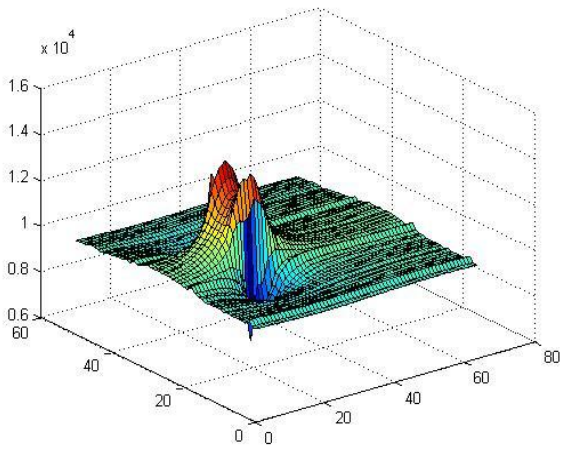

Fig 9e: Surface plot for 8 mm length variation

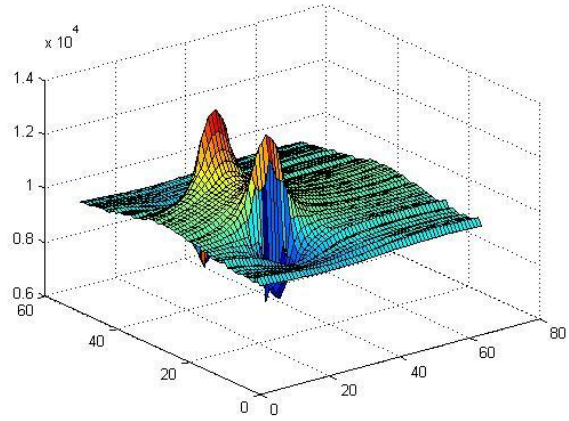

Fig 9f: Surface plot for 16 mm length variation

The impact of variation in the dimension of flaws on the MFL signal is shown in above plots 9(a)-9(f). One of the simplest ways to denote the 3D flux leakage profile is to plot the surface for the corresponding MFL signal. Any inhomogeneity of the tube surface is clearly indicated by the surface plot. The above Figures 9e and 9f illustrate the surface plot for length variation of defect geometry. The surface plots hold the information about the shape of the defect. Similar to the cut line plot shown in Figure 6a and 6b, the surface plot's upper portion varies depending upon the different shape of notches such as rectangular, elliptical and triangular.

6. CONCLUSION

The MFL is a useful tool that allows the rapid monitoring of large surface areas and corrosion pits. The signals and map plot of the MFL density were analysed. The magnetic flux density is calculated using COMSOL 4.3 for the SGTs of smaller diameter. The results show that the three dimensional (3D) analysis of geometry is an effective method to identify the flaws in ferromagnetic tubes of different dimensions. Several factors have an effect on flux discharge profiles owing to defects in the pipeline. These embrace operational variables and geometrical factors. The best approach to defect sizing is to build a database and use it for a defect characterisation. The intensity of the leakage field will increase with the rise in defect depth.

The pixel intensity variations in the resultant MFL images, which have been obtained from the proposed imaging system, clearly portray the information about the location and dimension of the artificial defects. The images obtained using this method may be used as the raw images in the image processing researches for characterizing the defects. This model will be very useful to conduct the simulation studies, which are required to fabricate an MFL imaging system, for the tubes of different diameter/wall thickness/material/defects.

7. ACKNOWLEDGMENTS

The authors would like to thank Board of Research in Nuclear Science (BRNS), Mumbai for funding the work, the collaborators Indira Gandhi Centre for Atomic Research (IGCAR), Kalpakkam for supporting this research, and Junior Research Fellow Mr. T. Senthil Kumar for his technical assistance.

8. REFERENCES

[1] Baldev Raj, Jayakumar.T, Thavasimuthu,M. 2002 Practical non-destructive testing. Narosa publishing house, New Delhi

[2] Yong Li, Gui Yun Tian, John Wilson 2007 Experiment and simulation study of 3D magnetic field sensing for magnetic flux leakage defect characterization. ELSEVIER, NDT&E, vol.40, pp.179-184.

[3] Andrew J. Lynch, 2009 Magnetic flux leakage robotic pipe inspection: internal and external methods. Dissertation, Rice University.

[4] S.S.Udpa, W.Lord, 1998 Magnetic flux leakage modeling for mechanical damage in transmission pipelines.IEEE transactions on magnetics, vol.34, no. 5, pp.3020-3023.

[5] Hiroaki Kikuchi, Kaito Sato, Isamu Shimizu, Yasuhiro Kamada and Satoru Kobayashi, 2011 Feasibility study of MFL to monitoring of wall thinning under reinforcing plates in nuclear power plants. IEEE transactions, vol.47, issue10, pp.3963-3966.

[6] Katragadda.G, Lord.W 1996 Alternative magnetic flux leakage modalities for pipe line inspection. IEEE transaction on magnetics, vol 32,no 3, pp.1581-1584.

[7] Neil R. Pearson, Matthew A. Boat, Robin. H. Priewald, Matthew J. Pate, John S. D. Mason, 2012 Practical capabilities of MFL in steel plate inspection. 18th World Conference on Nondestructive Testing, pp.16-20.

[8] Xiang LI, CHEN Liang, QIN Guangxu, FENG Peifu and HUANG Zuoying 2008 Steel pipeline testing using magnetic flux leakage method. IEEE transaction.

[9] Rao.B.P.C, Jayakumar.T 2012 Recent trends in electromagnetic NDE techniques and future direction.18th world conference on Nondestructive testing.

[10] Atzlesberger. J, Zagar.B.G 2011 Magnetic anomaly detection in ferromagnetic material. PIERS proceeding, pp.130-134.

[11] M.Li, D.A.Lowther, 2010 The application of topological gradients to defect identification in magnetic flux leakage type NDT. IEEE trans on magnetics, vol 46,no 8.

[12] Ahmad khodayari, James P.Reily, Natalia k Nikolova, 2009 Machine learning techniques for the analysis of magnetic flux leakage images in pipeline inspection. IEEE trans on magnetics vol 45, no 8

[13] Muhammad Afzal, Satish upda 2002 Advanced signal processing of magnetic flux leakage data obtained from seamless gas pipe line. NDT&E,pp.449-457

[14] Wong Toh Ming, 2004 Design and construction of magnetic flux leakage inspection System for ferro magnetic material. Dissertation, University of Technology Malaysia.

[15] Xinjun WU, Jiang XU, Yanling WANG, 2004 Signal processing methods for magnetic flux leakage testing based on bispectrum. Huazhong University of Science and Technology.

[16] Huang Zuoying, Que peiwen 2006 3D FEM analysis in magnetic leakage method. NDT&E, pp.61-66.

[17] Nathan Ida, William lord 1983 3D finite element prediction of magnetic leakage field. IEEE trans on magnetics vol 19 no 5

[18] Maryam Ravan, Reza Khalaj Amineh, 2010 Sizing of 3D arbitrary defects using magnetic flux leakage measurements. IEEE trans on magnetics, vol 46, no 4,

[19] Zulkarnay zhakariya, muhmad saiful badri mansor, 2010 Simulation of magnetic flux leakage analysis using FEMM. IEEE symposium on industrial electronics and application, pp.481-486.

[20] Rajesh T. Keshwani, 2009 Analysis of magnetic flux leakage signals of instrumented pipeline inspection gauge using finite element method. IETE Journal of Research, vol.55, issue 2, pp.73-81.

[21] Sharatchandra singh.W, Thirunavukkarasu.S, Mahadevan.S, Rao.B.P.C, Mukopadhyay, Jayakumar.T 2010 Three dimensional FEM of magnetic Flux Leakage technique for detection of defects in carbon steel plates. COMSOL conference

[22] Rajesh T. Keshwani, 2010 Three dimensional finite element modeling of magnetic flux leakage technique for detection of defects in carbon steel plates. COMSOL conference.

[23] COMSOL 4.3 Multiphysics modelling and simulation www.comsol.com